Stimulus-Driven Retinal Intrinsic Signal Optical Imaging in Mouse Demonstrates a Dominant Rod-Driven Component

Momotaz Begum, Dorothy P. Joiner, and Daniel Y. Ts'o

Department of Neurosurgery, SUNY Upstate Medical University, Syracuse, New York, United States

Correspondence: Daniel Y. Ts'o, Department of Neurosurgery, SUNY Upstate Medical University, 750 E. Adams Street, Syracuse, NY 13210, USA;
tsod@upstate.edu.

Received: July 22, 2019
Accepted: June 18, 2020
Published: July 28, 2020

Citation: Begum M, Joiner DP, Ts'o DY. Stimulus-driven retinal intrinsic signal optical imaging in mouse demonstrates a dominant rod-driven component. *Invest Ophthalmol Vis Sci.* 2020;61(8):37.
https://doi.org/10.1167/iovs.61.8.37

Purpose. The primary hypotheses tested are that (1) there exist stimulus-driven intrinsic optical signals in the mouse retina similar to those previously observed in other species, and (2) these optical signals require an intact rod photoreceptor phototransduction cascade.

Methods. We used 38 wild-type C57BL6J mice and 18 genetic knockout Gnat1$^{-/-}$ mice to study the light-evoked retinal intrinsic response. A custom mouse fundus camera delivered visual stimuli and collected mouse retinal imaging data of changes in retinal reflectance for further analysis. The retina was stimulated in the high-mesopic range with a 505-nm light-emitting diode while also being illuminated with 780-nm near-infrared light.

Results. Wild-type C57BL6J mice yielded retinal imaging signals that typically showed a stimulus-driven decrease in retinal reflectance of ~0.1%, with a time course of several seconds. The signals exhibit spatial specificity in the retina. Overall, the mouse imaging signals are similar in sign and time course to those reported in other mammalian species but are of lower amplitude. In contrast, functional retinal imaging of Gnat1$^{-/-}$ mice that lack a functional rod transducin yielded no such stimulus-driven signals.

Conclusions. Previous studies have not shown which pathway component is essential for the generation of these imaged signals. The absence of the intrinsic signal responses in Gnat1$^{-/-}$ knockout mice indicates that a functional rod transducin is likely to be necessary for generating the retinal intrinsic signals. These studies, to the best of our knowledge, demonstrate for the first time in vivo mouse retinal functional imaging signals similar to those previously shown in other mammalian species.

Keywords: intrinsic signal optical imaging, neurovascular coupling, rod transducin

The method of retinal intrinsic signal optical imaging (ISOI) has the potential to be a useful diagnostic tool in vision research and clinical settings to study the function of the retina in healthy and diseased states. Previous studies have shown stimulus-evoked changes in reflectance of retina in the human, macaque monkey, cat,[1–4] and other species. These intrinsic optical signals are thought to derive from various sources, including light scattering and hemodynamics.[5] The non-invasive retinal ISOI technique has been used in the cat extensively to study the biophysical origins of the stimulus-evoked retinal responses.[6–8] Our lab previously demonstrated that this decrement (negative change) in retinal reflectance in the cat is spatially correlated to the stimulus and dominated by a hemodynamic component.[6,7,9] A pharmacological blockade of the inner retina with tetrodotoxin and similarly at the level of postreceptoral retinal circuitry with 2-amino-4-phosphonobutyric acid and *cis*-2,3-piperidinedicarboxylic acid,[7] did not affect the spatial and temporal properties of stimulus-evoked intrinsic responses. The results of these experiments indicate that the signals originate in the outer retina. Bleaching studies[10] (Tso DY, et al. *IOVS* 2010;51:ARVO E-Abstract 1068) have also supported the notion that the intrinsic signals are dominated by the activity of rod photoreceptors. These studies showed that the time course of recovery and required spectrum for bleaching the retinal intrinsic signals matches that of the rod photopigment (recovery about 40–45 minutes). Furthermore, the action spectra of the signals themselves also match that of rhodopsin.[11] These findings indicate that the intrinsic signal responses originate in the outer retina, driven by the rod photoreceptors. Separately, studies using blood contrast agents in the cat have demonstrated that these signals are predominantly hemodynamic in nature.[8] A further determination of the precise cellular origins and neurovascular coupling mechanisms of these retinal intrinsic signals will be critical to establishing how these methods may find utility in specific clinical applications such as the diagnosis and management of particular retinal pathologies in human patients.

The central hypotheses of this study are

1. There exist measureable stimulus-driven intrinsic optical signals in the mouse retina that are similar to those previously observed in other species.
2. These optical signals require an intact rod photoreceptor phototransduction cascade.

We first sought to demonstrate the existence of stimulus-driven retinal intrinsic signals in the mouse retina. The mouse model promises to facilitate a greater range of investigations of the origins of these intrinsic signals and provide a platform to explore the effectiveness of retinal ISOI in the study of retinal pathology. We constructed a custom retinal imager to adapt this imaging technique to the mouse and demonstrate the presence of stimulus-driven retinal signals in the wild-type (WT) C57BL6J mouse retina. To further establish the role of rod photoreceptors in driving the generation of these retinal signals, we used a mouse knockout (KO) model, Gnat1$^{-/-}$, which lacks a functional rod transducin.[12] The rods of this KO mouse cannot generate an electrical (hyperpolarizing) light response and therefore would not be expected to yield retinal imaging signals under our current understanding of their origins.

The data presented here address two questions: (1) Is the retinal ISOI technique possible in mice? and (2) Given that the signals arise in the outer retina in other species, as previous results indicated, do the signals require the electrical response of the rod photoreceptors? In addition to these questions, we also have compared the mouse retinal signals to those found in other mammalian species. We did not seek to fully explore any possible functional signals originating from the cones but rather focused on matching the signals previously observed in these other species. Our results demonstrate for the first time, to the best of our knowledge, that the retinal intrinsic optical reflectance changes measured with flood illumination in the near-infrared also exist in the WT C57BLJ6 mouse retina in vivo, have a time course similar to those observed in cat and monkey retina, and are likely to be hemodynamic in origin. They are, however, weaker in amplitude. The mouse signals are also spatially specific but are not as well defined as those found in cat or monkey retina (greater point spread). Furthermore, we did not see any stimulus-driven retinal signal in the Gnat1$^{-/-}$ KO mouse retina, indicating that a functional rod transducin is necessary to generate these light-evoked retinal intrinsic responses.

Materials and Methods

Animals and Preparation

All experiments were conducted in accordance with the ARVO Statement for the Use of Animals in Ophthalmic and Vision Research and were approved by the SUNY Upstate Medical University Institutional Animal Care and Use Committee.

Male C57Bl/6J mice, 7 to 18 weeks old, served as wild-type controls. A colony of Gnat1$^{-/-}$ mice (a knockout strain lacking rod alpha-transducin) was generated from breeders obtained from Janis Lem, PhD (Tufts Medical Center, Boston, MA). Male and female Gnat1$^{-/-}$, ages 7 to 11 weeks, were also studied with retinal functional imaging. Previously, studies on this strain[12] have shown that their retinas are anatomically normal through 12 weeks of age, which we confirmed via postmortem retinal histology. A total of 56 mouse retinas (38 from WT mice and 18 from Gnat1$^{-/-}$) were used for the study, although population analyses were performed on a subset of 30 WT mice.

Mice were induced with ketamine/xylazine (126/12.6 mg/kg intraperitoneally [IP]). Anesthesia was maintained during the experiment by an initial dose of Nembutal, 12.5 mg/kg IP in the upper right abdomen[13] (Brent Bell, personal communication, Cole Eye Institute, Cleveland Clinic), followed by a constant infusion of Nembutal (2.5 mg/mL in saline) delivered IP using a 21-gauge butterfly catheter connected to a syringe pump (16.67 mg/kg per hour). Oxygen was delivered via a tube over the nose at a rate of 0.2 L/min throughout the experiment. This anesthetic protocol was chosen from a range of other tested agents, including periodic ketamine/xylazine injections, isoflurane, urethane, and variations thereof (imaging data collected under these other anesthetic protocols are not presented here). The chosen protocol exhibited the best stability of the anesthetic plane and suppression of body and eye movements without undue respiratory suppression over the relatively long recording period, often 6 hours or more. The Nembutal protocol was also closest pharmacologically to the barbiturate anesthetic protocols used in our prior cat[6] and macaque monkey retinal imaging studies, thus facilitating species comparisons (see below).

Atropine sulfate (1% for dilation) followed by phenylephrine (10% to prevent accommodation) ophthalmic drops were applied to both eyes. Body temperature was maintained throughout the experiment by a temperature-controlled heating pad set to 37.5°C, and the mouse was secured in a stereotaxic frame (David Kopf Instruments, Tujunga, CA, USA). A drop of proparacaine (0.5%) was applied to the ocular surface prior to placement of the retinal imager. The eyes were kept moist by frequently applying either an atropine/saline solution (1:5) or silicone oil (10,000 centistokes).

Mouse Endoscopic Retinal Imager

A custom mouse retinal imager was constructed, based in part on an endoscopic (otoscope) front end[14] but with optical paths similar to those described by Schallek et al.[6] Briefly, a 3-mm otoscope provided for separate imaging and concentric illumination light paths, facilitating construction of an economical mouse retinal imager. Its primary drawback is poor light efficiency. C-mount back-end components (Edmund Optics, Barrington, NJ, USA) incorporated a dichroic (cold) mirror to split the imaging path into a visible stimulus presentation path and a near-infrared (NIR) reflectance return path that ended with an objective lens, NIR long-pass filter (blocking shorter wavelength stimulus energy), and a charge-coupled device (CCD) camera (Fig. 1). The imaging field of view into the mouse retina was approximately 30°, and the imager was typically adjusted to bring the retinal vasculature into focus.

The retina was illuminated via a fiberoptic cable attached to the otoscope, which in turn was fed by NIR light (750–800 nm interference filter, typically 780 ± 30 nm) from a 100-W tungsten halogen source powered by a high-stability DC power supply (Kepco, Inc., Flushing, NY, USA). The tip of the endoscope was carefully positioned over and in contact with the mouse cornea. The visible stimulus was provided by a single green light-emitting diode (LED; 505 nm) with a focusing lens such that a focused image of the LED chip was projected onto the retina. Image acquisition runs consisted of blocks of trials of randomly interleaved stimulus and blank conditions. CCD camera (12-bit, Teledyne Photometrics, Tucson, AZ, USA) frame rates were typically 1 to 2 Hz, with a resolution of 192 × 144 pixels,[15] yielding about 7 pixels per degree. Images were acquired for a period of 10 to 20 seconds per trial, with an intertrial interval of 5 seconds. The acquisition software automatically rejected

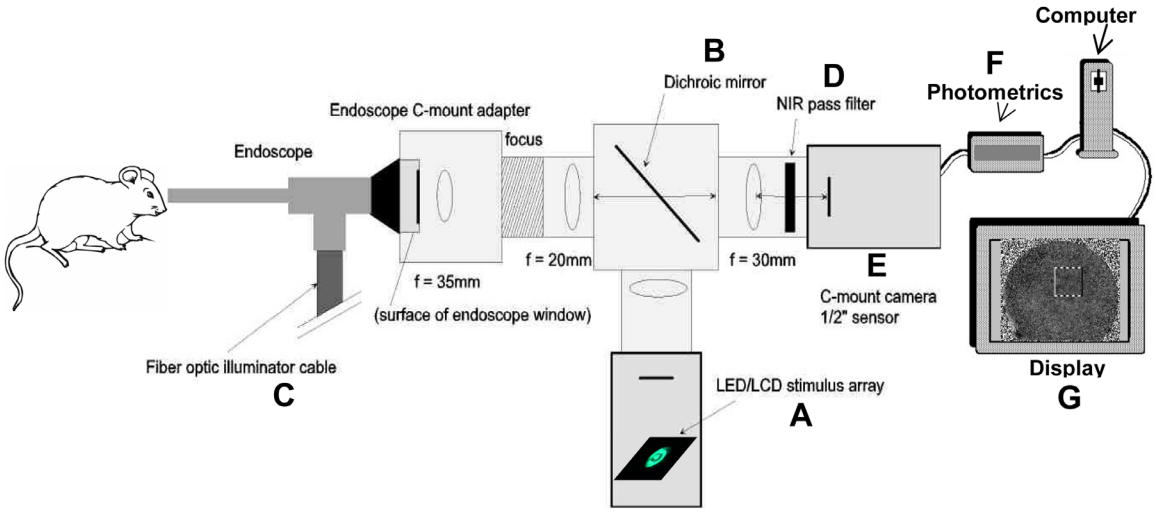

Figure 1. Diagram of modified mouse retinal optical imager. The mouse retinal imaging setup largely followed the same configuration as we have used with larger species, except that the commercial fundus camera has been replaced with a custom endoscopic imager. (**A**) A focused single *green* LED provides a patterned visual stimulus (the LED did not contain a diffuser, and the structure of the LED chip was clearly visible). (**B**) A dichroic mirror directs the visual stimulus into the optical pathway of the endoscopic retinal imager. (**C**) A tungsten halogen incandescent bulb is the source of illumination via a fiberoptic cable. (**D**) Illumination wavelengths are filtered by selected NIR filters. (**E**) NIR reflectance signals are collected by a cooled CCD camera, which sends data to a host computer (**F**) for data storage. (**G**) A display monitor shows the retinal image collected by the CCD camera.

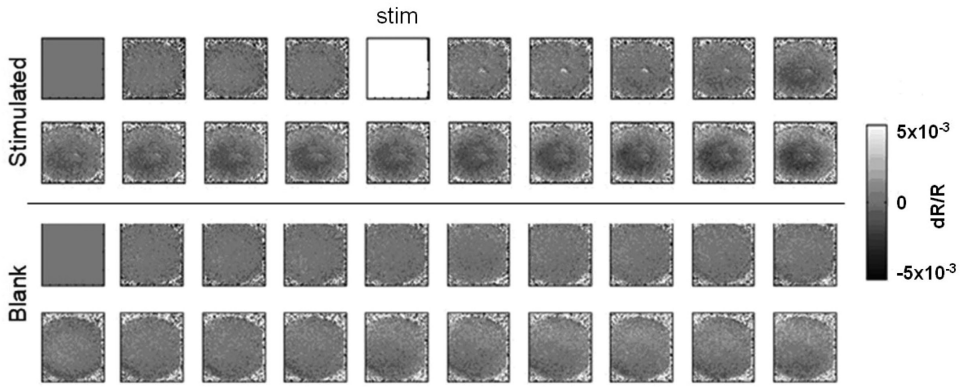

Figure 2. Time series of blank and stimulated mouse retinal images. The average of eight trials for blank and stimulus conditions (*green* LED) showing the grayscale images of fractional change in reflectance (dR/R) derived by dividing by the initial image ($t = 0$). A 300-ms stimulus pulse (stim) was delivered at the fifth frame (5 seconds). Images were acquired at a rate of one per second. Notice the response after stimulus presentation versus blank condition. The stimulus used saturated the CCD camera for that (*white*) frame, due to leak-through of the dichroic mirror used in this experiment.

and discarded trials that contained movement artifacts. The recording sessions typically lasted over 6 hours and were conducted in the dark. The stimulus intensity (luminance) was set to be 8 to 20 cd/m^2, in the high mesopic range, by adjusting the current into the LED, with a pulse duration of 300 ms. Spatial location of the stimulus could also be controlled by positioning the LED off-center and rotating the LED holder.

Image Analysis

The data analysis was done by a custom computer analysis program.[15] Our analysis examined the time course and the spatial properties of the intrinsic signal response. A 40 × 40-pixel region of interest (ROI) within the stimulated or non-stimulated retina was used to assess the amplitude of the pre- and post-stimulus change in reflectance (dR/R).[6] The optical signals reported are then fractional reflectance changes—that is, reflectance changes normalized to the resting or pre-stimulus retinal reflectance, which is determined by averaging the initial 2 seconds of pre-stimulus reflectance. All retinal images of the intrinsic signal in the figures after Figure 2 are computed based on the dR/R analysis integrated over 8 seconds immediately post-stimulus. Error bars in the figures represent the SEM. The observed, stimulus-driven negative dR/R, a reduction in reflectance, is typical of an increase in hemoglobin absorption due to functional hyperemia.[8,9,16]

Investigative Ophthalmology & Visual Science

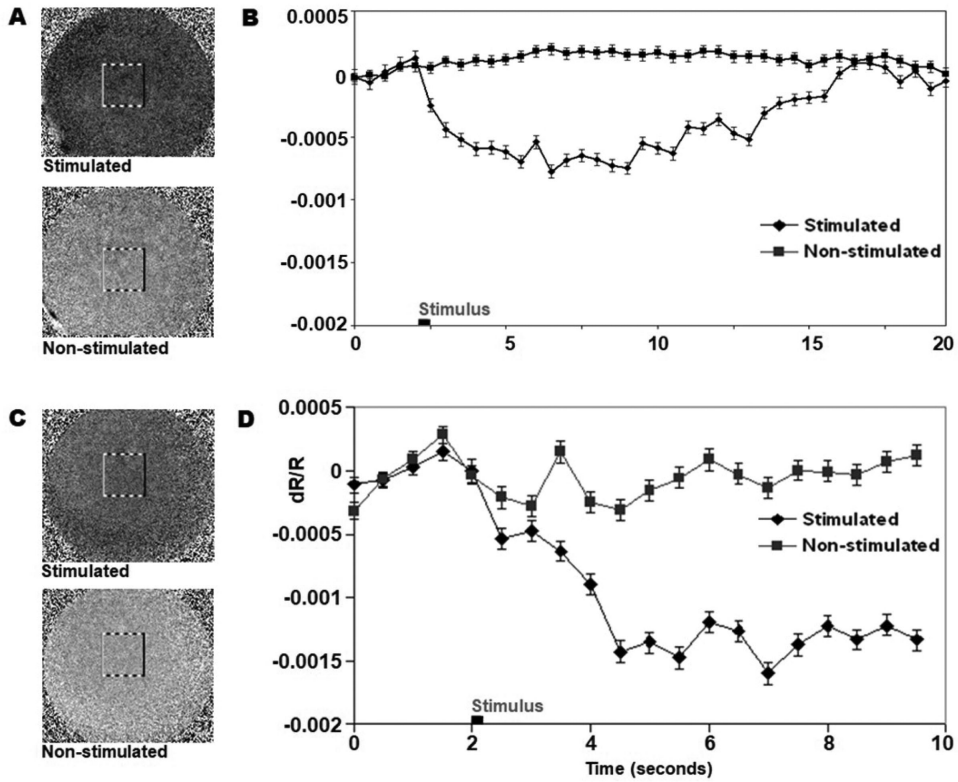

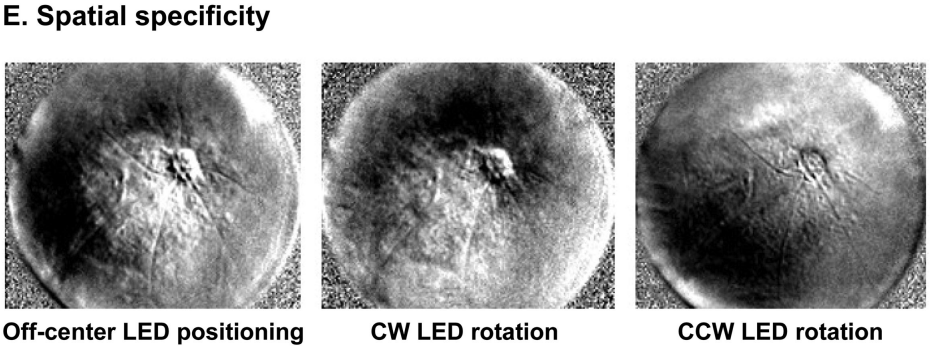

Figure 3. WT C57BL6J intrinsic responses. Intrinsic signal optical imaging is demonstrated in mice. (**A**, **C**) Examples of NIR (780 nm) images of the fundus of two individual WT mice with a *green* LED spot flash (stimulated, *top*) and without stimulus (non-stimulated, bottom). The dashed square denotes the ROI. (**B**, **D**) Magnitude and time courses for fractional change in reflectance (dR/R) of the selected ROIs from the images in **A** and **C** (*boxed areas*). Zero to 2 seconds is the pre-stimulus period. At 2 seconds, the stimulus was presented for 300 ms (dark bar on the *x*-axis in **B** and **D**) for the stimulated condition. In **B** and **D**, the time courses are plotted out to 20 and 10 seconds, respectively. Error bars show the SEM over 12 repetitions. (**E**) Spatial specificity of the intrinsic response as shown by displacement of the stimulated region with a clockwise and a counterclockwise rotation of an eccentric (*off-center*) stimulus LED, as compared with the retinal response prior to the rotations (*leftmost*). A shallow depth of field reveals greater detail of the retinal vasculature. Note the differences in time scale shown in **B** and **D**. The pixel noise seen outside of the imaged fields is due to fixed pattern noise of the CCD sensor.

Results

Light Stimulus-Induced Intrinsic Signal Response in WT Mouse Retina

To demonstrate activity-dependent intrinsic optical signals in mouse retina similar to those described in other species, we conducted retinal imaging trials using WT mice. Shown in Figure 2 is a time series of the NIR reflectance images of the retinal response to a 300-ms green (505 nm) LED spot stimulus covering an approximately 20° portion out of the 30° of the imaged retina, as compared with the blank (no stimulus) condition. Plotting of the time course (Fig. 3A) of the changes in reflectance dR/R in a ROI before and after the flash stimulus revealed a light-evoked retinal intrinsic response similar to that described in previous studies of other species. The WT mouse retina showed a consistent negative reflectance after the stimulus onset (following a 2-second pre-stimulus period). Two examples from two individual mice are shown in Figure 3, with each plot showing data from 12 repetitions. Activation of the retina with the green LED visual spot stimulus resulted in an overall darkening (negative reflectance change at 780 nm) of the retinal image as compared with the unstimulated retinal image

Investigative Ophthalmology & Visual Science

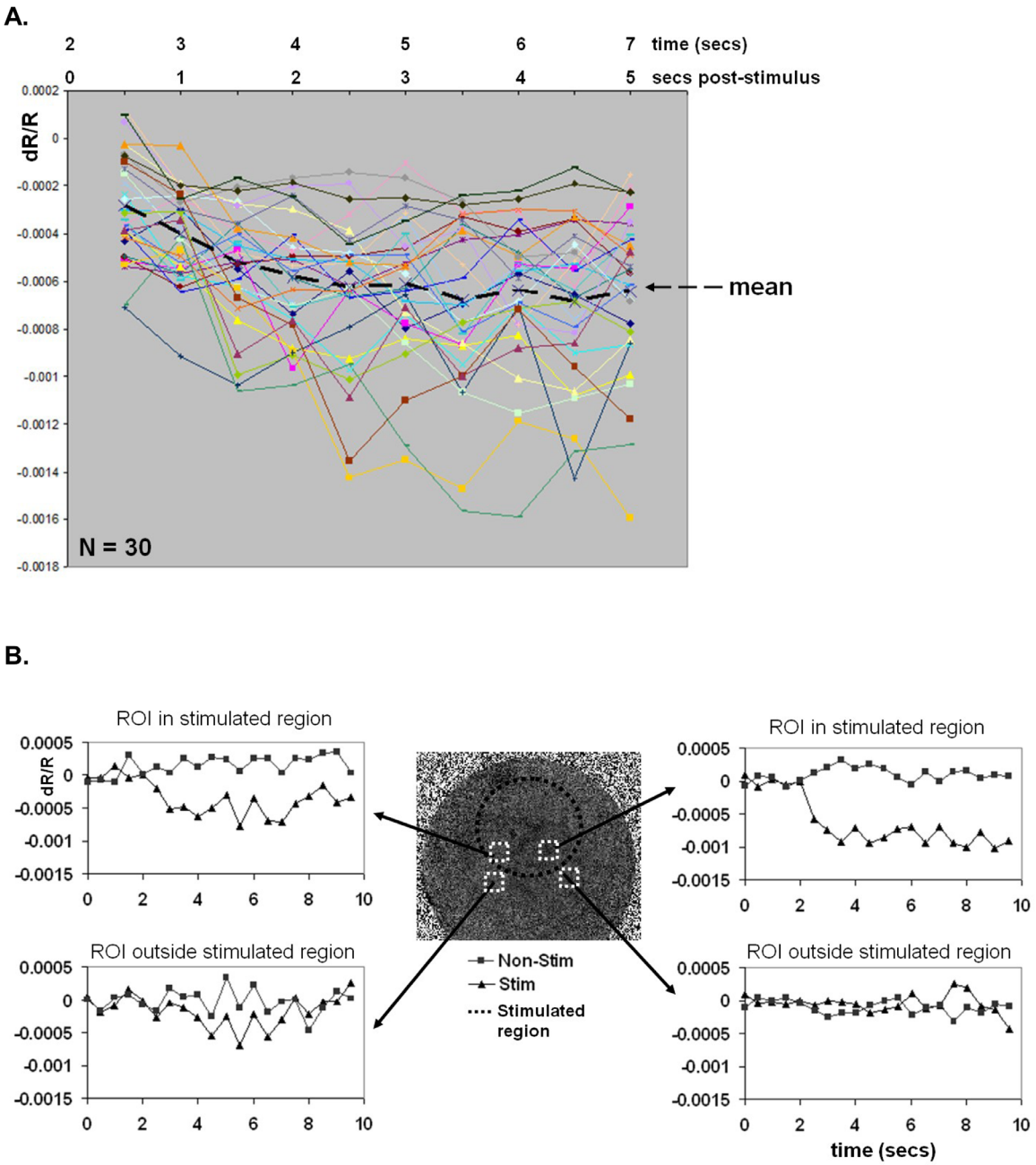

Figure 4. Variability of mouse retinal intrinsic functional signals. (**A**) Time slice of multiple ($N = 30$) stimulated retinal intrinsic signals, beginning 0.5 seconds post-stimulus, for 5 seconds, showing the variability among 30 individuals, as well as their mean (*heavy dashed line*) peak amplitude of $-0.64 \times 10^{-3} \pm 0.31 \times 10^{-3}$ (SD). (**B**) Amplitude and time course of the response from two ROIs (top plots) located within the stimulated region, recorded concurrently, as well as two ROIs (bottom plots) located just outside the stimulated region, also recorded concurrently.

(Figs. 3A, 3C). The intensity of the presented stimuli were not sufficient to yield appreciable photopigment bleaching (which would be a positive-signed signal due to the reduction in absorbed light). The sign of the imaged signals (negative reflectance) also cannot be explained by a direct stimulus artifact, which would have also yielded a positive signal.

Time Course of the Intrinsic Response in WT Mice

To quantify the time course of the retinal intrinsic response, we analyzed ROIs (40 × 40-pixel regions in Figs. 3A and 3C) from stimulated and non-stimulated conditions imaged in WT C57BL6J mice and determined the fractional reflectance change (dR/R). The magnitudes of the dR/R within these ROIs from both stimulated and non-stimulated states were plotted as a function of time (Figs. 3B, 3D). The ROIs from the non-stimulated retinal image showed insignificant deviation from baseline reflectance (zero on the *y*-axis) as seen by the dR/R for Figures 3B and 3D, and they are stable throughout the imaging period. In the stimulated condition, there was negligible deviation from the baseline during the first 2 seconds (pre-stimulus period). At stimulus onset

Investigative Ophthalmology & Visual Science

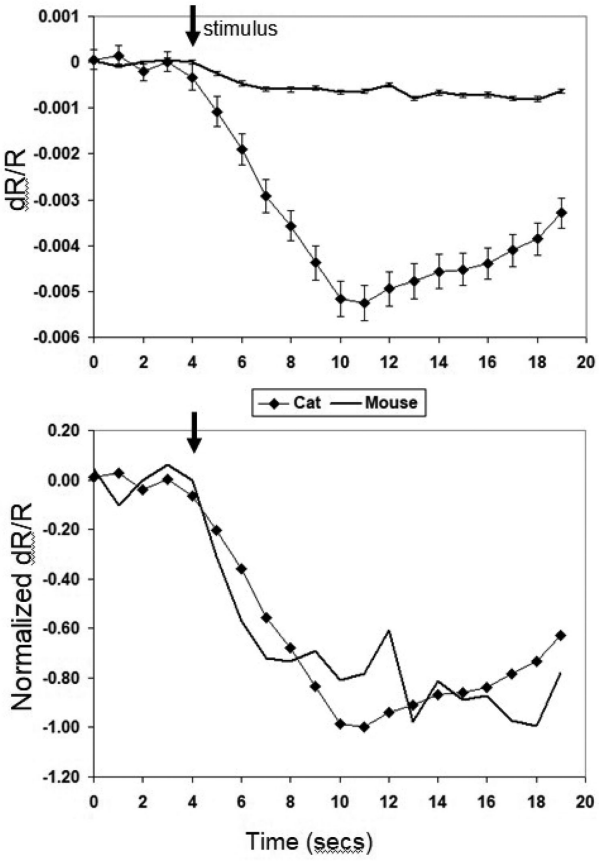

Figure 5. Comparison of cat and mouse retinal intrinsic functional signals. Amplitude and time course of the response from example individuals from each species when stimulated with the same *green* stimulus luminance (8 cd/m^2). In the bottom plot, the responses have been normalized to their respective peak values to better show the similarity of the time courses. The primary difference between the two species is the larger fractional reflectance change in the cat. Error bars show the SEM.

(2 seconds), the retina was stimulated with a green LED spot stimulus. A negative change in reflectance was observed that monophasically developed over the initial 2 seconds following the stimulus and then reached a plateau; the response amplitude persisted for several seconds. It was then followed by a slow recovery which took over 10 seconds to return to the baseline (Fig. 3B, plotted out to 20 seconds). These results demonstrate the presence of a stimulus-driven intrinsic optical signal in mouse retina that bears much similarity to that previously described in other mammalian species.[6,17] Figure 4A presents multiple signal plots for 5 seconds post-stimulus, from 30 mice, showing the individual variability of the retinal intrinsic signals, as well as a mean peak amplitude of $-0.64 \times 10^{-3} \pm 0.31 \times 10^{-3}$ (SD). A post hoc power analysis indicated that 12 mice would have been sufficient to achieve significance of the observed results.

One difference between these mouse retinal signals and those found in cat retina is that a spatially separate positive dR/R signal was sometimes observed in cat retina,[6] but we only observed a negative dR/R for C57BL6J mice (Fig. 5). The signal amplitudes observed in the mouse retina were also roughly an order of magnitude smaller compared to the retinal signal seen in the cat (Fig. 5) for the same stimulus luminance and were typically in the range of 0.5 to 1.5×10^{-3} (negative fractional reflectance change, –dR/R).

Spatial Properties of the Intrinsic Signals in WT C57BL6J Mice

Although an overall darkening of the mouse retinal image in the stimulated conditions was observed following the stimulus, further analysis revealed a regional specificity within the stimulated condition that is spatially correlated with placement of the stimulus on the retina. Figure 3E illustrates the spatial specificity of the intrinsic response to an eccentric (off-center), spatially restricted green LED spot stimulus that was rotated to shift the stimulus position, resulting in a corresponding shift in the spatial pattern of the retinal response. Analysis of ROIs chosen from stimulated and non-stimulated retinal regions (Fig. 4B) further demonstrated a spatial specificity of the imaged functional signals.

Spatial and Temporal Properties of ISOI Signals in Gnat1$^{-/-}$ Mouse Retina

To further establish the origins and mechanisms underlying the retinal functional imaging signals, we compared the stimulus-driven signals in the WT mouse retina with those recorded in the retina of the Gnat1$^{-/-}$ KO mouse, a strain that is missing a functional rod transducin.[12] The imaging paradigm and analysis were identical for the WT C57BL6J and Gnat1$^{-/-}$ KO mouse retinal imaging studies. If the retinal intrinsic signals of the mouse are rod driven, then imaging the retina of the Gnat1$^{-/-}$ KO mouse should show no negative dR/R dip with light stimulation.

Example responses from two Gnat1$^{-/-}$ mice retina are shown in Figure 6. In contrast to the stimulus-evoked darkening that was apparent in the stimulated conditions of WT C57BL6J retinal images (Figs. 3A, 3C), we observed no stimulus response in retinal imaging from the Gnat1$^{-/-}$ retina, as seen in Figures 6A and 6C. The imaged signals between the stimulated and non-stimulated conditions were indistinguishable. To further investigate the existence of the functional intrinsic signal in the retina of Gnat1$^{-/-}$, we quantified the dR/R ($n = 18$) for the selected ROIs from the Gnat1$^{-/-}$ retinal imaging. Two examples are shown in Figures 6B and 6D. There was no change in reflectance before or after the stimulus onset at 2 seconds for the Gnat1$^{-/-}$ mice in the stimulated condition. The time course of the response magnitude (expressed as dR/R) from the non-stimulated ROI is similar to the response magnitude of the stimulated condition (Figs. 6B, 6D). This observation was evident when the mean Gnat1$^{-/-}$ ($n = 18$) dR/R was compared with the mean responses from WT C57BL6J retina ($n = 30$). Figure 7A illustrates the amplitude and time course of the mean intrinsic responses for the WT C57BL6J mouse, and Figure 7B displays the mean intrinsic responses of the Gnat1$^{-/-}$ KO mouse. C5BL6J mouse retinas ($n = 30$) showed a consistent negative reflectance dip immediately after the stimulus onset. No such consistent, rapid negative reflectance dip is seen in Gnat1$^{-/-}$ KO mice ($n = 18$). The results from these experiments support the notion that the light-evoked retinal response is of outer retinal origin and is rod dominated, requiring the electrical response of rod photoreceptors for intrinsic signal generation.

Investigative Ophthalmology & Visual Science

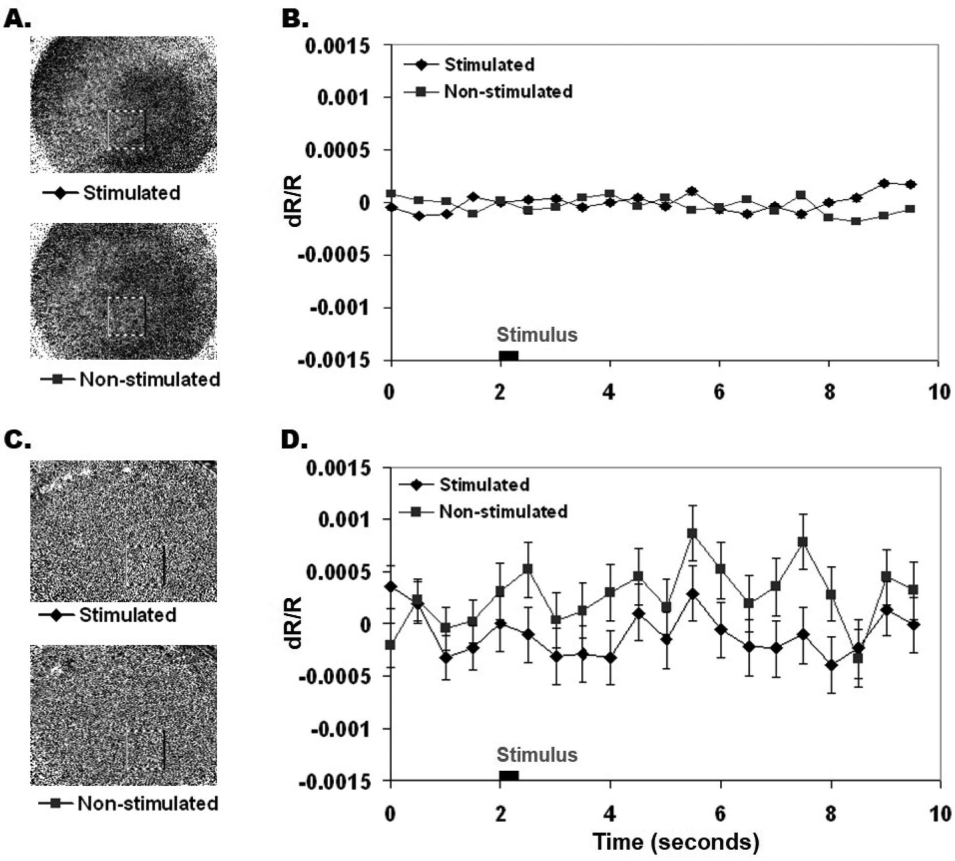

Figure 6. Retinal intrinsic signal in a transducin knockout. (**A**, **C**) Spatial properties of the intrinsic response; two examples of NIR ISOI images of Gnat1$^{-/-}$ mouse retinas. (**B**, **D**) Magnitude and time courses for fractional change in reflectance (dR/R) of the selected ROIs from the images in **A** and **C**. Zero to 2 seconds is the pre-stimulus period. At 2 seconds, the stimulus was presented for 300 ms (dark bar on the *x*-axis in **B** and **D**) for the stimulated condition and no stimulus for non-stimulated condition. These examples show no stimulus-driven functional retinal signal (ISOI) in the Gnat1$^{-/-}$ mouse. Error bars show the SEM.

Discussion

In this study we have demonstrated stimulus-driven intrinsic optical signals in the mouse retina using ISOI. As with several other mammalian species examined, this response to a visual stimulus imaged in mouse retina is a negative reflectance (dR/R) signal in the NIR, with a time course that is similar to signals in human, cat, and monkey retina. However, the magnitude of the response observed in mouse retina is smaller than in these other species.[3,6] Perhaps related, the point spread function of the imaged response in mouse is also greater. What accounts for these differences? Although it is difficult to be certain about the contributing factors given the information available, several considerations may be pertinent. One obvious species difference is the presence of a tapetum in the cat, which may have at least two forms of impact on the amplitude of the retinal intrinsic signals. First, the nature of the vasculature underneath the cat's tapetum differs from that of mouse and primate retinas and suggests a possible impact on the properties of the neurovascular coupling mechanisms and oxygen delivery to the stimulated retina. Indeed, its presence may impede the effectiveness of the choroid circulation and shift the reliance of the outer retina toward the retinal circulation. In addition, the tapetum is thought to contribute to a marked increase in the light sensitivity of the cat retina, although other retinal mechanisms beyond "double-chance reflection" are required to fully explain the extent of the sensitivity boost. Some optical imaging studies in mouse neocortex have suggested that the mouse neurovascular coupling mechanisms overall may be less effective than in cat and primate. Thus, the observation of a lower amplitude and spatial precision of the stimulus-driven intrinsic signals in mouse retina may be a consequence of some combination of these issues raised, although further studies are required to address these ideas.

Previous studies in cats have demonstrated the intrinsic signal is driven by rod photoreceptors and dominated by hemodynamics.[7] The pharmacological studies determined that the driving response is in the outer retina, prior to the photoreceptor/bipolar cell synapse. These studies showed that the imaged signals remained with the blockade of either inner retinal activity or the photoreceptor synapse itself but lacked a demonstration of just what component was required, without which the signals were abolished. Here, we investigated the role of the rod transducin on the intrinsic signal using a specific transgenic mouse model, Gnat1$^{-/-}$, and have shown that the signals are abolished in the absence of a functional rod transducin. There were no dR/R optical signals after stimulus onset in Gnat1$^{-/-}$ retina, indicating that the signal requires the phototransduction cascade of rod photoreceptors and that a functional rod transducin is essential for the generation of the intrinsic signal. This

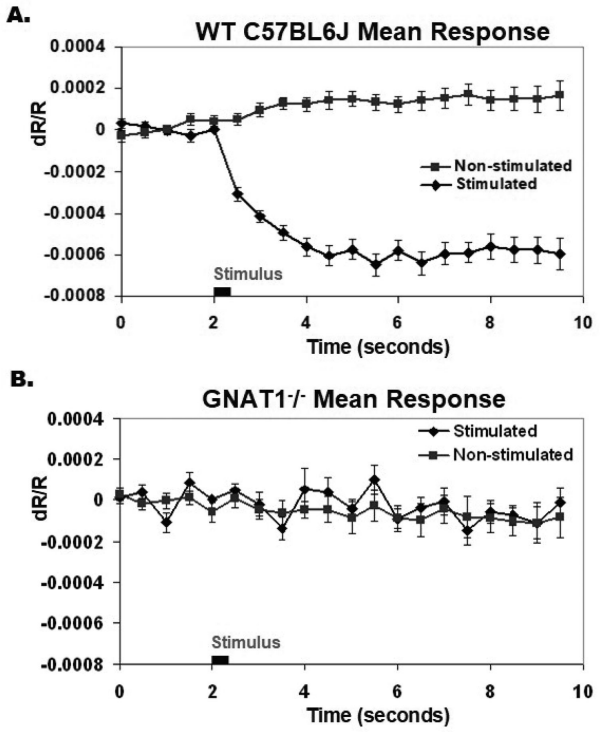

Figure 7. Mean responses of WT and KO mice. (**A**) Mean responses of WT C57BL6J ($N = 30$) to a spot *green* LED flash. (**B**) Mean responses of Gnat1$^{-/-}$ ($n = 18$; to a same stimulus as **A**). In contrast to the WT mouse, no stimulus-driven functional retinal signal is seen in the Gnat1$^{-/-}$ KO mouse. Error bars show the SEM.

result further supports the notion that the intrinsic response is dominated by the activity of rod photoreceptors. Although these results are not surprising given previous findings in other mammalian species,[6,7] they do rule out a strong contribution from the melanopsin intrinsically photosensitive retinal ganglion cells[18] as a possible alternative mechanism for light transduction of the imaged stimulus-driven retinal signals. Although there may be smaller contributions from other phototransduction mechanisms,[19] at the high mesopic light levels tested the rods are dominant, a finding that has been supported by previous studies.[10,11,20] Although weaker cone signals may exist and might be revealed by changes in the imaging protocols, preliminary attempts to uncover such signals using light-adapted, rod-saturating backgrounds and photopic stimuli have been equivocal. As the rod photoreceptor population far outnumbers the cones, most previous efforts, including this study, have focused on these robust signals at mesopic stimulus levels.

A potential confound in the use of the Gnat1$^{-/-}$ KO is the reported increase in oxidative stress in this mouse strain,[21] thus allowing the possibility that oxidative stress may contribute to the absence of the intrinsic optical signals in Gnat1$^{-/-}$. Although it is known that oxidative stress can impact the neurovascular unit, the effects are likely to be incremental,[22] whereas the absence of the stimulus-driven intrinsic optical signals is complete, mirroring the absence of rod phototransduction[12] in Gnat1$^{-/-}$. Diabetic mice with elevated oxidative stress beyond that observed in Gnat1$^{-/-}$ still have functioning rod phototransduction, and the level of increase in oxidative stress in Gnat1$^{-/-}$ as measured by superoxide production is not clear (perhaps only +20%).[21] Thus, it is still more parsimonious to conclude that the results seen in Gnat1$^{-/-}$ are primarily due to the absence of rod phototransduction. Further studies are needed to clarify this complex issue.

The stimulus-driven intrinsic optical signals in the mouse retina reported here parallel signals previously described in other species measured under similar conditions. Studies indicate that these signals are hemodynamic in origin and are driven by the outer retina. They are one class of a constellation of activity-driven retinal intrinsic signals that differ in spectral properties, sign, amplitude, time course, and underlying biophysical mechanisms.[23,24] Other examples include much faster light-scattering signals that are most apparent in hemoglobin-free in vitro measurements[23] and much slower signals (10–100-second rise times) described in OCT studies[25,26] that appear to be driven by osmotic mechanisms.[26] The measurement of these slow signals is conducted at wavelengths (840–860 nm) where hemoglobin absorption is low, and hemodynamic signals may be further reduced from a confounding oximetry signal of the opposing sign. Thus, differences in time course, spectral properties, and measurement methodologies suggest multiple signal classes of differing origins and mechanisms.

Combined with previous studies demonstrating the persistence of these imaged retinal signals with a blockade of the photoreceptor/bipolar synapse, the implied chain of events, from visual stimulus to the imaged changes in retinal reflectance, would seem to include (1) rod phototransduction; (2) non-neural signaling at the photoreceptor synapse, likely involving the Müller cells; and (3) alterations of neurovascular coupling leading to the imaged hemodynamics. These steps are supported and consistent with studies on the complex biochemical cascades underlying neurovascular coupling and the role of retinal glia.[27–29]

Because our study demonstrates intrinsic signal retinal functional imaging in the mouse, it opens up a more general application of the method to retinal research that would benefit from a relatively economical assessment of retinal function. The rich variety of mouse KO strains that exhibit altered retinal development, structure, function, and health creates the opportunity to study various retinal disease models using ISOI. Many retinal disorders have direct and indirect consequences on the retinal vasculature; therefore, their study may be aided by an imaging technique that is sensitive to the neurovascular function of the retina.

Acknowledgments

The authors thank Sandra McGillis, Eduardo Solessio, Peter Calvert, and Ronald A. Miller for their help with data collection and/or review of the manuscript.

Supported by a National Institutes of Health Grant (NIH/EB002843).

Disclosure: **M. Begum,** None; **D.P. Joiner,** None; **D.Y. Ts'o,** None

References

1. Abramoff MD, Kwon YH, Ts'o D, et al. Visual stimulus-induced changes in human near-infrared fundus reflectance. *Invest Ophthalmol Vis Sci*. 2006;47:715–721.
2. Barriga ES, Pattichis M, Ts'o D, et al. Spatiotemporal independent component analysis for the detection of functional responses in cat retinal images. *IEEE Trans Med Imag*. 2007;26:1035–1045.

3. Tsunoda K, Oguchi Y, Hanazono G, Tanifuji M. Mapping cone- and rod-induced retinal responsiveness in macaque retina by optical imaging. *Invest Ophthalmol Vis Sci*. 2004;45:3820–3826.
4. Hanazono G, Tsunoda K, Shinoda K, Tsubota K, Miyake Y, Tanifuji M. Intrinsic signal imaging in macaque retina reveals different types of flash-induced light reflectance changes of different origins. *Invest Ophthalmol Vis Sci*. 2007;48:2903–2912.
5. Malonek D, Grinvald A. Interactions between electrical activity and cortical microcirculation revealed by imaging spectroscopy: implications for functional brain mapping. *Science*. 1996;272:551–554.
6. Schallek J, Li H, Kardon R, et al. Stimulus-evoked intrinsic optical signals in the retina: spatial and temporal characteristics. *Invest Ophthalmol Vis Sci*. 2009;50:4865–4872.
7. Schallek J, Kardon R, Kwon Y, Abramoff M, Soliz P, Ts'o D. Stimulus-evoked intrinsic optical signals in the retina: pharmacologic dissection reveals outer retinal origins. *Invest Ophthalmol Vis Sci*. 2009;50:4873–4880.
8. Schallek J, Ts'o D. Blood contrast agents enhance intrinsic signals in the retina: evidence for an underlying blood volume component. *Invest Ophthalmol Vis Sci*. 2011;52:1325–1335.
9. Ts'o D, Schallek J, Kwon Y, Kardon R, Abramoff M, Soliz P. Noninvasive functional imaging of the retina reveals outer retinal and hemodynamic intrinsic optical signals origins. *Jpn J Ophthalmol*. 2009;53:334–344.
10. Schallek J, Ts'o DY. Intrinsic signals of the retina reveal a rod-driven component consistent with dark adaptation time course. Society for Neuroscience Program No. 403.1. *2009 Neuroscience Meeting Planner*. Washington, DC: Society for Neuroscience; 2009.
11. Ts'o DY, Schallek JB. The scotopic action spectra of intrinsic signals of the retina reveal a rod-driven mechanism. Society for Neuroscience Program No. 171.8. *2010 Neuroscience Meeting Planner*. Washington, DC: Society for Neuroscience; 2010.
12. Calvert PD, Krasnoperova NV, Lyubarsky AL, et al. Phototransduction in transgenic mice after targeted deletion of the rod transducin alpha-subunit. *Proc Natl Acad Sci USA*. 2000;97:13913–13918.
13. Bell BA, Kaul C, Rayborn ME, Hollyfield JG. Baseline imaging reveals preexisting retinal abnormalities in mice. In: LaVail MM, Ash JD, Anderson RE, Hollyfield JG, Grimm C, eds. *Retinal Degenerative Disease*. New York: Springer-Verlag;2012:459–469.
14. Paques M, Guyomard J-L, Simonutti M, et al. Panretinal, high-resolution color photography of the mouse fundus. *Invest Ophthalmol Vis Sci*. 2007;48:2769–2774.
15. Ts'o DY, Frostig RD, Lieke EE, Grinvald A. Functional organization of primate visual cortex revealed by high resolution optical imaging. *Science*. 1990;249:417–420.
16. Frostig RD, Lieke EE, Ts'o DY, Grinvald A. Local coupling between cortical activity and microcirculation revealed by high-resolution in vivo optical imaging. *Proc Natl Acad Sci USA*. 1990;87:6082–6086.
17. Tsunoda K, Hanazono G, Inomata K, Kazato Y, Suzuki W, Tanifuji M. Origins of retinal intrinsic signals: a series of experiments on retinas of macaque monkeys. *Jpn J Ophthalmol*. 2009;53,297–314.
18. Berson DM, Dunn FA, Takao M. Phototransduction by retinal ganglion cells that set the circadian clock. *Science*. 2002;295:1070–1073.
19. Allen AE, Cameron MA, Brown TM, Vugler AA, Lucas RJ. Visual responses in mice lacking critical components of all known retinal phototransduction cascades. *PLoS One*. 2010;5:e15063.
20. Ts'o DY, Schallek JB. Chromatic bleaching reveals a rod-driven component in retinal intrinsic optical signals. *Invest Ophthalmol Vis Sci*. 2010;51:1068.
21. Liu H, Tang J, Du Y, et al. Transducin1, phototransduction and the development of early diabetic retinopathy. *Invest Ophthalmol Vis Sci*. 2019;60:1538–1546.
22. Carvalho C, Moreira PI. Oxidative stress: a major player in cerebrovascular alterations associated to neurodegenerative events. *Front Physiol*. 2018;9:806.
23. Yao X, Wang B. Intrinsic optical signal imaging of retinal physiology: a review. *J Biomed Opt*. 2015;20:090901.
24. Hunter JJ, Merigan WH, Schallek JB. Imaging retinal activity in the living eye. *Annu Rev Vis Sci*. 2019;5:15–45.
25. Son T, Wang B, Thapa D, et al. Optical coherence tomography angiography of stimulus evoked hemodynamic responses in individual retinal layers. *Biomed Opt Exp*. 2016;7:3151–3162.
26. Zhang P, Zawadzki RJ, Goswami M, et al. In vivo optophysiology reveals that G-protein activation triggers osmotic swelling and increased light scattering of rod photoreceptors. *Proc Natl Acad Sci USA*. 2017;114:E2937–E2946.
27. Newman EA. Functional hyperemia and mechanisms of neurovascular coupling in the retinal vasculature. *J Cereb Blood Flow Metab*. 2013;33:1685–1695.
28. Ts'o DY, Begum M. Noninvasive functional retinal imaging disrupted by pharmacologic manipulation of neurovascular coupling pathways. *Invest Ophthalmol Vis Sci*. 2015;56:4123.
29. Begum M, Ts'o DY. Photoreceptor glial signaling during neurovascular coupling underlying functional retinal imaging. Program No. 238.07. *2016 Neuroscience Meeting Planner*. Washington, DC: Society for Neuroscience, 2016.

Investigative Ophthalmology & Visual Science